Cardiovascular Research (2013) **99**, 566–575
doi:10.1093/cvr/cvt081

Nerves projecting from the intrinsic cardiac ganglia of the pulmonary veins modulate sinoatrial node pacemaker function

Manuel Zarzoso[1,2], Kristina Rysevaite[3], Michelle L. Milstein[1], Conrado J. Calvo[1], Adam C. Kean[1], Felipe Atienza[4], Dainius H. Pauza[3], José Jalife[1], and Sami F. Noujaim[1,5]*

[1]Center for Arrhythmia Research, University of Michigan, Ann Arbor, MI, USA; [2]Universitat de València, Valencia, Spain; [3]Institute of Anatomy, Lithuanian University of Health Sciences, Kaunas, Lithuania; [4]Department of Cardiology, Hospital General Universitario Gregorio Marañón, Madrid, Spain; and [5]Molecular Cardiology Research Institute, Tufts University School of Medicine, Tufts Medical Center, 800 Washington Street, PO Box 8684, Boston, MA 02111, USA

Received 17 October 2012; revised 7 March 2013; accepted 28 March 2013; online publish-ahead-of-print 3 April 2013

Time for primary review: 33 days

Aims Pulmonary vein ganglia (PVG) are targets for atrial fibrillation ablation. However, the functional relevance of PVG to the normal heart rhythm remains unclear. Our aim was to investigate whether PVG can modulate sinoatrial node (SAN) function.

Methods and results Forty-nine C57BL and seven Connexin40$^{+/EGFP}$ mice were studied. We used tyrosine-hydroxylase (TH) and choline-acetyltransferase immunofluorescence labelling to characterize adrenergic and cholinergic neural elements. PVG projected postganglionic nerves to the SAN, which entered the SAN as an extensive, mesh-like neural network. PVG neurones were adrenergic, cholinergic, and biphenotypic. Histochemical characterization of two human embryonic hearts showed similarities between mouse and human neuroanatomy: direct neural communications between PVG and SAN. In Langendorff perfused mouse hearts, PVG were stimulated using 200–2000 ms trains of pulses (300 μs, 400 μA, 200 Hz). PVG stimulation caused an initial heart rate (HR) slowing (36 ± 9%) followed by acceleration. PVG stimulation in the presence of propranolol caused HR slowing (43 ± 13%) that was sustained over 20 beats. PVG stimulation with atropine progressively increased HR. Time-course effects were enhanced with 1000 and 2000 ms trains ($P < 0.05$ vs. 200 ms). In optical mapping, PVG stimulation shifted the origin of SAN discharges. In five paroxysmal AF patients undergoing pulmonary vein ablation, application of radiofrequency energy to the PVG area during sinus rhythm produced a decrease in HR similar to that observed in isolated mouse hearts.

Conclusion PVG have functional and anatomical biphenotypic characteristics. They can have significant effects on the electrophysiological control of the SAN.

Keywords Sinoatrial node • Intrinsic cardiac ganglia • Pulmonary veins

1. Introduction

The intrinsic cardiac nervous system comprises ganglionated nerve plexi located intramurally in the atria and ventricles.[1,2] Intracardiac ganglia are formed by heterogeneous populations of neural elements that include not only cholinergic postganglionic neurones, but also adrenergic, afferent, and interconnecting local circuit neurones.[3,4] The number of ganglia found in the heart is variable and species-dependent.[5] In many mammals, including humans, intrinsic cardiac ganglia are usually distributed at specific atrial regions around the sinoatrial node (SAN), the roots of caval and pulmonary veins, and near the atrioventricular node.[6,7] More specifically, it has been shown that the general morphology of the mouse cardiac ganglionated nerve plexus is similar to those in larger mammals, including humans.[2]

It has been suggested that intrinsic cardiac ganglionated plexi exert influence over adjacent myocardial regions.[8–10] The SAN can be regulated by intrinsic ganglia located in its vicinity and this regulation has been assumed to be mainly parasympathetic.[11–14] Ablation of the pulmonary vein ganglia (PVG) has been proposed as a therapy for atrial fibrillation.[15] On the other hand, pulmonary vein isolation has been shown to affect

* Corresponding author. Tel: +1 617 636 5190; fax: +1 617 636 4833, Email: sami.noujaim@tufts.edu

heart rate (HR) variability and acceleration and deceleration capacity of HR, due to the possible destruction of PVG, indicating that PVG are active in the control of HR.[15] However, the role that these remotely located ganglia can have in SAN modulation is not completely understood.

Our main objective was to test the hypothesis that PVG can contribute to the control of the SAN pacemaker function. Accordingly, we used immunohistochemistry, electrical stimulation, and optical mapping in mouse hearts to examine the intrinsic innervation of SAN and the PVG and the modulation of the SAN by PVG stimulation. We also examined PVG–SAN innervation in human foetal hearts and quantified the effects of radiofrequency energy application (RFA) to the antrum of pulmonary veins on HR.

2. Methods

An expanded section is available in Supplementary material online, Detailed Methods. Animal-handling protocols were in accordance with the animal care guidelines of the European Union (2010/63/EU) and the National Institutes of Health Guidelines for the Care and Use of Laboratory Animals (NIH publication, 8th edition, 2011). All procedures were approved by the University of Michigan Committee on Use and Care of Animals (UCUCA) and the Kaunas Bioethical Committee.

2.1 Immunohistochemistry and microscopic examination

We used tyrosine-hydroxylase (TH) and choline-acetyltransferase (ChAT) immunofluorescence labelling to characterize, respectively, adrenergic and cholinergic structures in whole-mount mouse atrial preparations as described previously.[2] Additional studies were performed in two embryonic human hearts by means of acetylcholinesterase.[5] The investigation conforms to the principles outlined in the Declaration of Helsinki.

2.2 Electrophysiological study in mice

In Langendorff perfused hearts, PVG were stimulated using high-frequency stimulation (300 μs, 400 μA, 200 Hz) with 200–2000 ms trains of pulses. Volume-conducted electrocardiograms were recorded to assess the effects of PVG stimulation at the roots of the pulmonary veins on the mouse SAN activity by measuring changes in the P–P interval. In additional experiments, the effect of chemical stimulation of the PVG was studied with local application of nicotine (Supplementary material *Figure S3*).[3]

2.3 Optical mapping

Epicardial optical mapping was performed in isolated hearts and in isolated superfused atrial preparations of wild-type C57BL and $Cx40^{+/EGFP}$ mice.[16] Recording rate was 1 kHz, and resolution 75 μm/pixel. Activation maps were constructed before and, for the first beat, after PVG stimulation.

2.4 Human electrophysiological study

We analysed five paroxysmal AF patients who underwent ablation for PV isolation. All patients gave informed consent. The investigation was approved by the ethics committee of Hospital General Universitario Gregorio Marañón. The three-dimensional geometry of the left atrium and PVs was constructed using electroanatomical mapping systems, and RF current was applied around the PV antrum of the patients. ECG was analysed to assess the RFA effects on P–P interval.

2.5 Statistical analysis

Values are reported as mean ± SD unless stated otherwise. Repeated measures analysis of variance with the Bonferroni test for multiple comparisons and paired *t*-test were used when appropriate (SPSS, version 17.0 for Windows). Differences were considered significant at a two-tailed $P < 0.05$.

3. Results

3.1 Neuroanatomical characterization of the whole-mount atrial preparation

PVG and SAN areas were exposed, and the atria flattened. Cholinergic structures labelled with ChAT antibodies were visualized in the red channel (*Figure 1A*). Adrenergic structures labelled with TH antibodies are in green (*Figure 1B*). *Figure 1C* shows both red and green channels simultaneously. The PVG are located at the roots of the pulmonary veins, and form a circuit via interconnecting nerve fibres. Nerves emerge from the ganglionic circuit and advance towards the SAN area (white arrows), suggesting neuroanatomical communication between the PVG and the SAN. We examined in further detail the structure and the innervation of the intact mouse SAN (Supplementary material online, *Figure S1*) and the PVG. *Figure 1D–F* shows a characterization of the PVG. *Figure 1E* and *F* shows the image of the ChAT and TH staining, respectively. They are merged in *Figure 1D*. These ganglia are biphenotypic since both sympathetic and parasympathetic somas are present within the same ganglion. Nerves advancing from these ganglia contain both sympathetic and parasympathetic axons. Given the nature of these ganglia, the degree of SAN innervation, and the anatomical connection between the PVG and the SAN shown in *Figure 1*, we proceeded to study the effects of stimulating these ganglia on HR and the activation of the SAN.

3.2 PVG stimulation and selective pharmacological blockade

In *Figure 2*, we compare the short-term effects of PVG stimulation on the P–P interval with those of right atrial appendage (RAA) stimulation. Three P–P intervals post-stimulation were averaged. In control (*Figure 2A*), stimulation of the PVG increased the spontaneous cycle length from 219 ± 21 ms pre-stimulation to 296 ± 34 ms post-stimulation ($P < 0.05$). This increase was statistically significant for all trains delivered. In *Figure 2B*, a similar increase in cycle length was observed (239 ± 2 ms pre-stimulation vs. 341 ± 30 ms post-stimulation; $P < 0.05$) when the stimulation was performed in the presence of propranolol. When the train duration increased to 1000, 1250, 1500, and 2000 ms, the increase in P–P interval became more pronounced ($P < 0.05$ vs. 200 ms, *Figure 2E*). In *Figure 2C*, the mean value of the first three P–P intervals tended to decrease when the PVG stimulation was carried out in the presence of atropine for the longest trains of stimulation (1250 and 2000 ms, $P < 0.05$ vs. pre-stimulation). In the atropine + propranolol group, P–P interval remained unchanged after PVG stimulation (*Figure 2D*). No differences in P–P interval were observed before stimulation between trains within each group, indicating that the time interval for recovery used between trains was sufficient for the pacemaker cycle to return to baseline. Likewise, RAA stimulation did not affect cycle length. This confirms that the stimulation used was subthreshold for atrial myocardium excitation (*Figure 2A–C*) and is consistent with what was shown before.[17,18] When we plotted *Figure 2A–D* as percentage increase in P–P with respect to pre-stimulation vs. the stimulation train duration (*Figure 2E*), no differences were observed between PVG stimulation in control and PVG stimulation in the presence of propranolol.

We computed the time-course of P–P interval changes for PVG stimulation in control, in the presence of propranolol or atropine. *Figure 3A–C* shows the increase in P–P interval for the first 20 beats

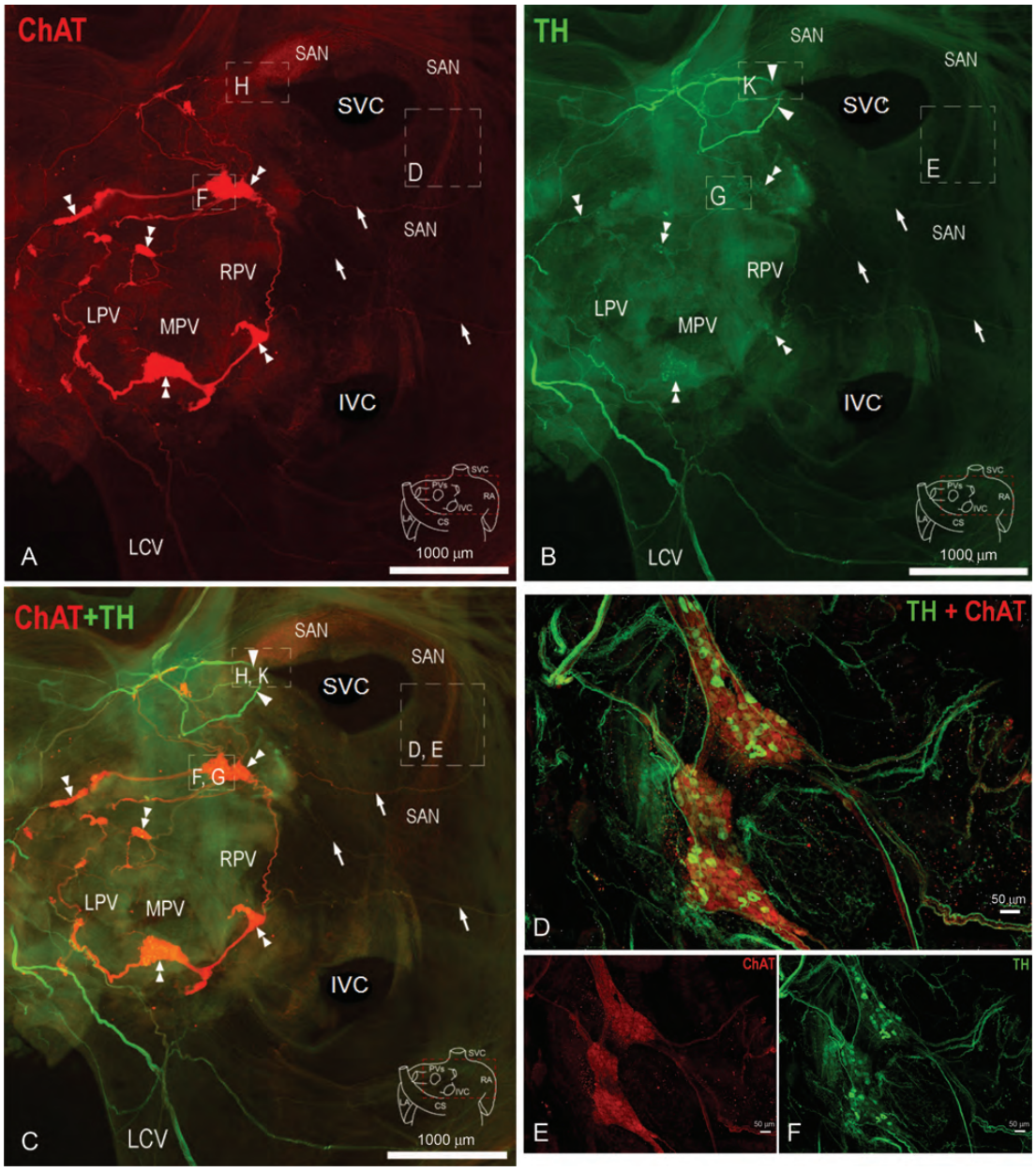

Figure 1 Neuroanatomical characterization of the mouse whole-mount atrial preparation and PVG (*A*–*C*). Arrowheads indicate extrinsic nerves accessing the mouse heart, whereas double arrowheads point to intrinsic ganglia located at the roots of PVs. Arrows indicate nerves emerging from the PVG, which extend to the SAN region. Boxed areas are enlarged in Supplementary material online, *Figure S1*. (*D*–*F*) Characterization of the PVG (green, TH; red, ChAT). LCV, left cranial vein; LPV, left pulmonary vein; MPV, middle pulmonary vein; RPV, right pulmonary vein; CS, coronary sinus.

after stimulation, expressed as percentage of the pre-stimulation P–P intervals. We used the shortest (200 ms), intermediate (1000 ms), and longest trains (2000 ms) for this analysis. In Supplementary material online, *Figure S2*, we show traces of ECG changes with PVG stimulation. In *Figure 3A*, for 200 ms trains, the time-course of the response in control was similar to that in the presence of propranolol, and a slight P–P interval shortening was observed for beats 13–20 in the presence of atropine. In *Figure 3B*, for 1000 ms trains, the effects of PVG stimulation on the P–P interval were accentuated, and statistically different among the three groups ($P < 0.01$, PVG stimulation vs. propranolol group vs. atropine group). PVG stimulation with propranolol resulted in an increase in cycle length that was maintained for 20 beats, whereas in the PVG group the initial increase in P–P interval was followed by significant acceleration after the 10th beat. In the atropine group, the decrease in P–P interval occurred immediately after stimulation and increased progressively towards a steady state. As shown in *Figure 3C*, for the longest train duration (2000 ms), the time-course response was also different among all three experimental groups ($P < 0.001$; PVG stimulation vs. propranolol group vs. atropine group; *Figure 3C*), following similar trends as with the 1000 ms trains. When complete autonomic blockade was achieved, P–P interval remained unchanged after PVG stimulation (*Figure 3A*–*C*).

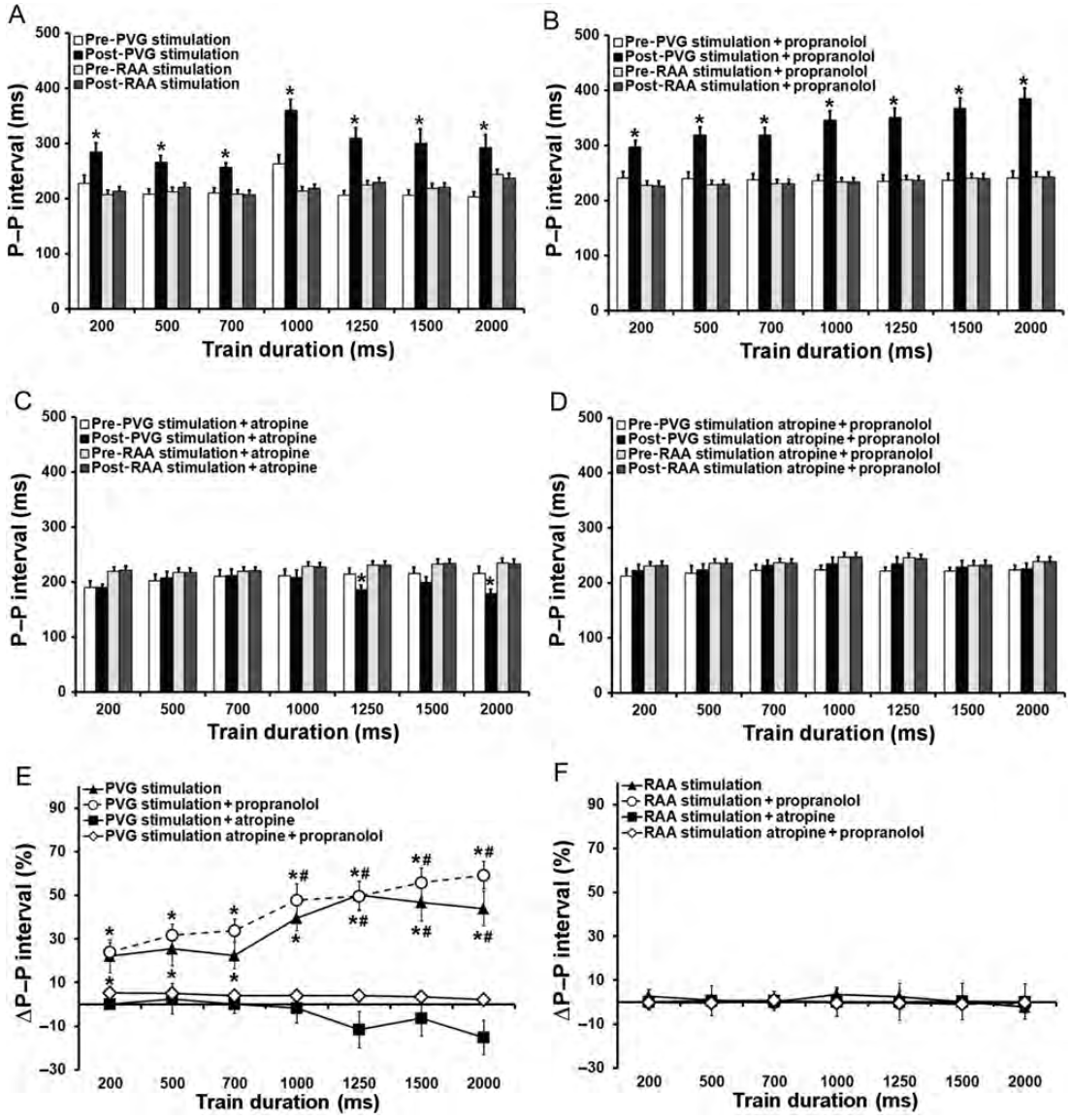

Figure 2 Immediate effects (average of three P–P intervals post-stimulation) of PVG stimulation on HR. (*A*) PVG stimulation ($n = 12$); RAA stimulation ($n = 23$); $^{*}P < 0.05$ vs. pre-stimulation. (*B*) PVG stimulation + propranolol ($n = 17$); RAA stimulation + propranolol ($n = 24$); $^{*}P < 0.05$ vs. pre-stimulation. (*C*) PVG stimulation + atropine ($n = 13$); RAA stimulation + atropine ($n = 16$); $^{*}P < 0.05$ vs. pre-stimulation. (*D*) PVG stimulation atropine + propranolol ($n = 16$); RAA stimulation atropine + propranolol ($n = 16$); (*E*) $^{*}P < 0.05$ vs. PVG stimulation + atropine and PVG stimulation atropine + propranolol; $^{\#}P < 0.05$ vs. 200 ms train.

3.3 Modulation of the SAN activation by PVG stimulation

We performed epicardial optical mapping of the right atrium in eight mice to assess whether a change in the leading pacemaker site occurred after PVG stimulation. In 78.1% of 25 observations before stimulation, spontaneous sinus rhythm activation originated near the SVC, where the SAN is traditionally found. In other cases ($n = 7$, 21.9%), the leading pacemaker site was closer to the IVC. In all hearts, the optical action potential duration at baseline was significantly longer in the SAN region than in the RAA (Supplementary material online, *Figure S4*).

After applying a 1000 ms train, the cycle length increased from 209 ± 21 ms to 338 ± 73 ms ($P < 0.05$ vs. pre-stimulation, $N = 8$ hearts, $n = 32$ observations) and the leading pacemaker site shifted in 22 out of 32 observations (68.8%). *Figure 4* illustrates data from two representative experiments in which PVG stimulation produced an upward shift (*Figure 4A*) and a downward shift (*Figure 4B*). PVG stimulation decreased the optical APD_{50} in the RAA (Supplementary material online, *Figure S7*) from 14.4 ± 2.7 to 11.9 ± 2.5 ms ($P < 0.001$ vs. pre-stimulation; $n = 32$ observations).

3.4 Isolated atria experiments

To further characterize the origin and shift in SAN activation post-PVG stimulation, we mapped isolated atrial preparations in three $Cx40^{+/EGFP}$ mice. After PVG stimulation (1000 ms train), the cycle length increased from 204 ± 29 to 333 ± 82 ms ($P < 0.05$ vs. pre-stimulation, $N = 3$ hearts, $n = 10$ observations; *Figure 5A*). Single-pixel recordings from

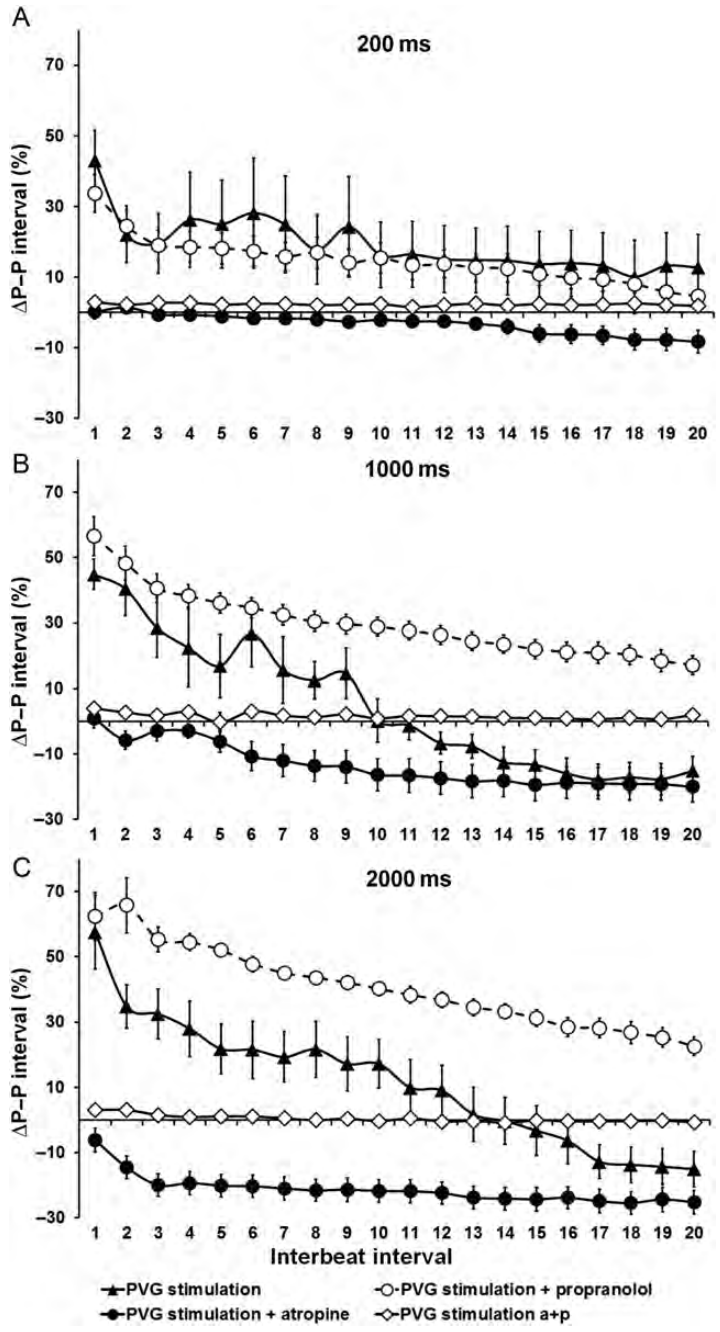

Figure 3 Time-course effects (20 beats after stimulation) of PVG stimulation with (*A*) 200 ms train, (*B*) 1000 ms train, and (*C*) 2000 ms train. PVG stimulation ($n = 12$); PVG stimulation + propranolol ($n = 17$); PVG stimulation + atropine ($n = 12$); PVG stimulation atropine + propranolol ($n = 16$).

the SAN area in *Figure 5C* before (black) and after stimulation (red) are shown in *Figure 5A*. We did not observe statistically significant differences in cycle length between experiments in the whole heart and those in isolated atria preparations, either during spontaneous sinus rhythm (209 ± 21 vs. 204 ± 29 ms; NS) or after PVG stimulation (338 ± 73 vs. 368 ± 79 ms; NS).

PVG stimulation caused either a shift (70%; $n = 7$) or no change (30%; $n = 3$) in the origin of SAN discharges. *Figure 5B* is a superimposition of the confocal scan of EGFP fluorescence onto the fluorescent image of the preparation during optical mapping. The SAN artery is visible, and the SAN area is bordered by the EGFP-positive atrial myocytes. A downward pacemaker shift occurred in 85.7% of observations (six out of seven). *Figure 5C* shows the initial activation of the SAN with respect to the SAN artery. *Figure 5D* depicts the downward shift in the origin of the leading pacemaker site post-PVG stimulation. Nevertheless, the location of the leading pacemaker remained confined to the SAN area.

3.5 Neuroanatomy of the human embryonic atria

We analysed 15-week-old human embryonic hearts stained with the Karnovsky–Roots acetylcholinesterase precipitation reaction as

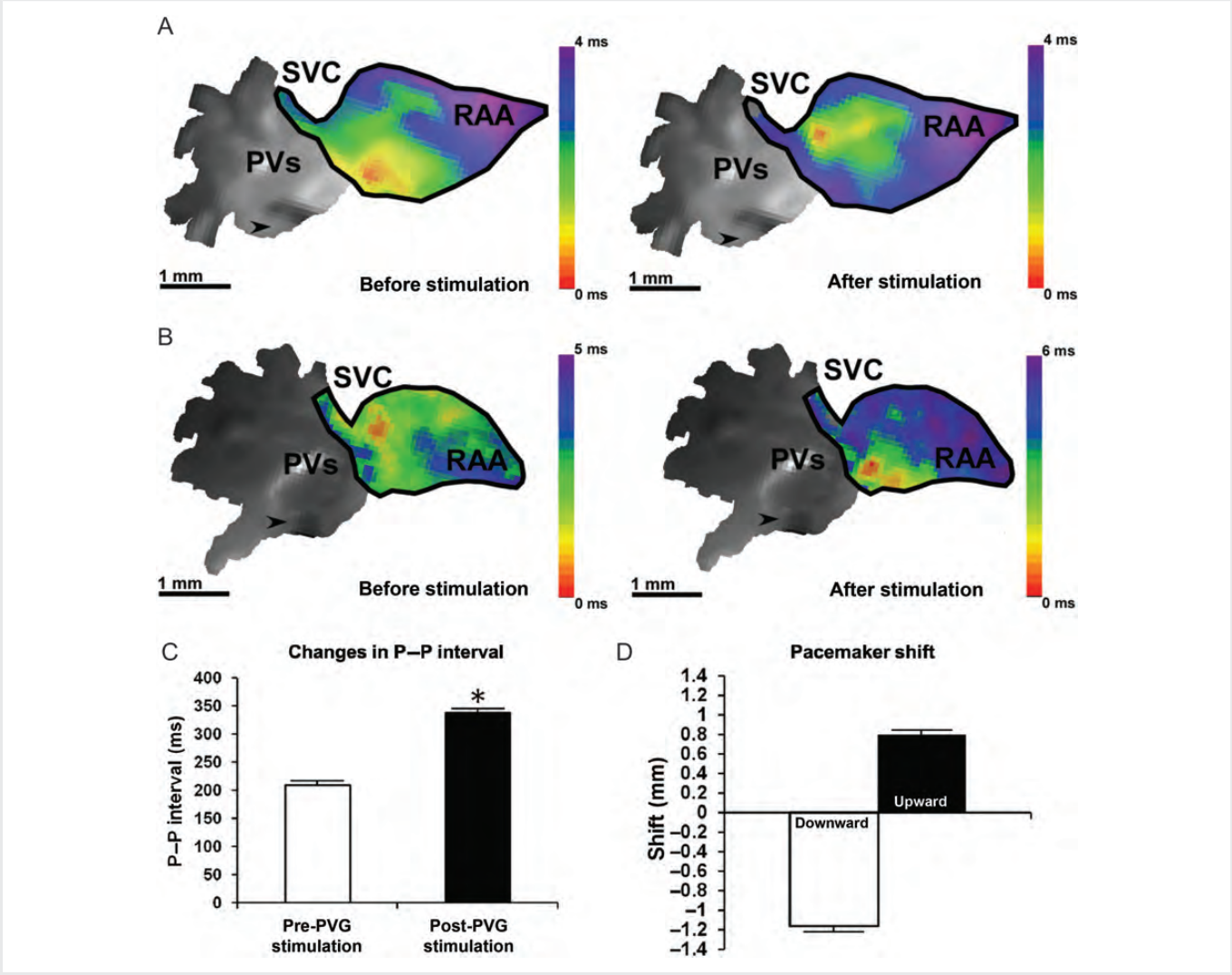

Figure 4 Modulation of the SAN activation pattern induced by PVG stimulation. The leading pacemaker site shifted upwards (*A*) in 31.8% of observations (seven of 22), after applying 1000 ms train of stimulation to the PVG. (*B*) A representative example of a downward shift after PVG stimulation. This took place in 68.2% of observations (15 of 22). (*C*) The increase in cycle length after 1000 ms trains. The quantification of the shift in the site of earliest activation is in (*D*). $N = 8$ hearts, $n = 32$ observations. SVC, superior vena cava; PV, pulmonary veins; RAA, right atrial appendage; arrows point towards the tip of the stimulation electrode. Colour bars in (*A*) and (*B*) display the activation time in milliseconds.

described previously.[19] We paid particular attention to the PVs/SAN regions (see also Supplementary material online, *Figure S8A*). *Figure 6A* shows direct neural communications between PVG and SAN, similar to the mouse heart (*Figure 1A–C*). These data support our contention that direct neural communications exist between PVG and the SAN.

3.6 Electrophysiological study in patients

We investigated the effects of RFA during sinus rhythm in five patients with paroxysmal AF (58 ± 6 years old, three males and two females) undergoing PV isolation. Patients' characteristics are shown in Supplementary material online, *Figure S8B*. *Figure 6C* and *D* shows maps illustrating three-dimensional geometry of the left atrium and PVs. The red arrows indicate the location of RFA at the roots of the left superior pulmonary vein (LSPV, *Figure 6C*) and the right inferior pulmonary vein (RIPV, *Figure 6D*). RFA at those specific sites led to HR slowing because of the likely stimulation of PV ganglia. The ECG recordings are shown in *Figure 6E*. The top tracings (leads II and V_5) show the time-course of HR changes in response to RFA at the LSPV and the bottom panel shows the effects of RFA delivery at the RIPV. Quantification of the changes in HR produced by RFA is presented in *Figure 6B*. The basal HR was computed as the mean of four beats immediately before RFA. The durations of 12 P–P intervals that followed RFA were plotted. After RFA delivery, there was an initial decrease in HR followed by acceleration towards basal HR. This response was similar to that observed in isolated mouse hearts (*Figure 3*).

4. Discussion

We used histochemistry, electrical stimulation, and optical mapping in mice, and electrophysiological studies in AF patients undergoing PV isolation to provide mechanistic insight into the regulation of SAN by the intracardiac ganglia at the roots of the pulmonary veins. The results can be summarized as follows: (i) PVG contain both adrenergic and cholinergic somas that project their axons to the SAN; (ii) PVG stimulation

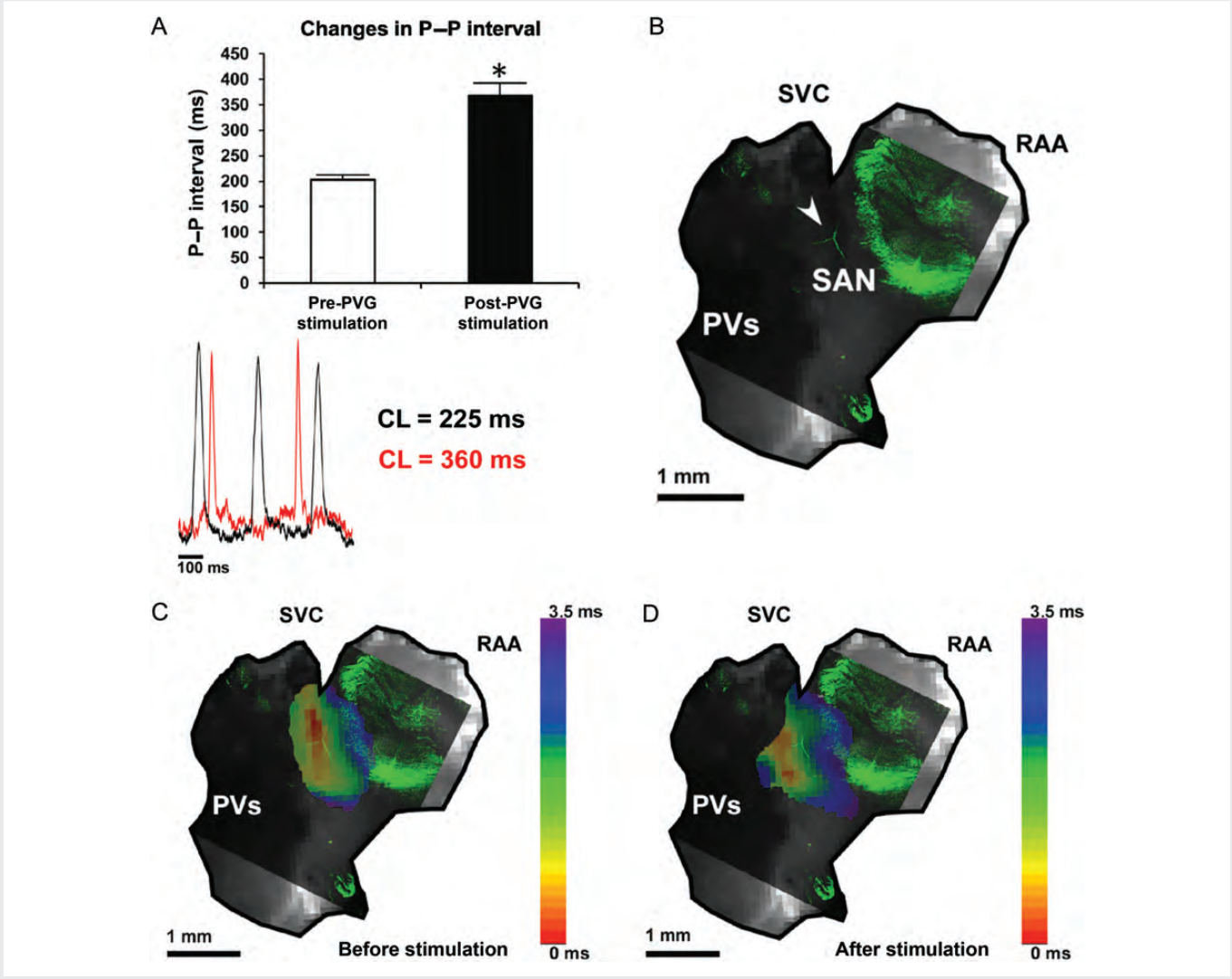

Figure 5 Combined EGFP fluorescence microscopy and optical mapping in isolated atrial preparation from Cx40$^{+/EGFP}$ mice. (*A*) PVG stimulation produced an increase in the P–P interval ($P < 0.05$ vs. pre-stimulation, top of the panel). Representative traces of a single pixel from the SAN area on (*C*) are shown before (black) and after stimulation (red). (*B*) EGFP fluorescence image of the SAN superimposed on the optical image of the atrial preparation. The white arrow points to the SAN artery. Activation maps showing the site of earliest activation with respect to the SAN artery before (*C*) and after PVG stimulation (*D*). Colour bars in (*C*) and (*D*) display the activation time in milliseconds.

can have significant effects on the discharge rate of the SAN without the need of extracardiac neural reflexes; (iii) pharmacological blockade uncovered a functional parasympathetic and sympathetic role of the PVG; (iv) stimulation of these ganglia can shift the dominant pacemaker location of the SAN; and (v) direct radiofrequency application at the roots of PV in patients slows the HR similar to PVG stimulation in isolated mouse hearts.

4.1 Neuroanatomy of PVG and SAN

Traditionally, intracardiac ganglionic neurones have been considered to be cholinergic, responsible for the second relay of parasympathetic fibres to the heart. Nevertheless, anatomical evidence revealed the presence of adrenergic neurones in the mammalian intrinsic cardiac ganglia.[20–22] In the present study, we showed that the PVG contain both adrenergic and cholinergic neurones (*Figure 1*). We observed strong similarities in the PVG neuroanatomical structure of humans (*Figure 6A*) and mice (*Figure 1*); in both humans and mice, PVG are located at the roots of the PVs. Most importantly, in both species, nerves emerge from the ganglionic circuit and advance towards the right atrium to richly innervate the SAN region and provide a direct neuroanatomical communication between the PVG and the SAN. Mabe and Hoover,[23] using confocal scans of murine SAN stained for vesicular acetylcholine (ACh) transporter and TH, reported the presence of noradrenergic and cholinergic nerves. This was also shown in the dog and rabbit SAN.[18,24] In those studies, tissue sectioning was done. In contrast, our data illustrate the undisturbed neuroanatomy of the intact SAN and provide the first evidence for neuroanatomical connections between the PVG and the SAN.

4.2 Effects of PVG stimulation on SAN automaticity

The initial effect of PVG stimulation (first three P–P intervals post-simulation) can be considered predominantly parasympathetic (*Figure 2A*). Furthermore, there were no differences between PVG

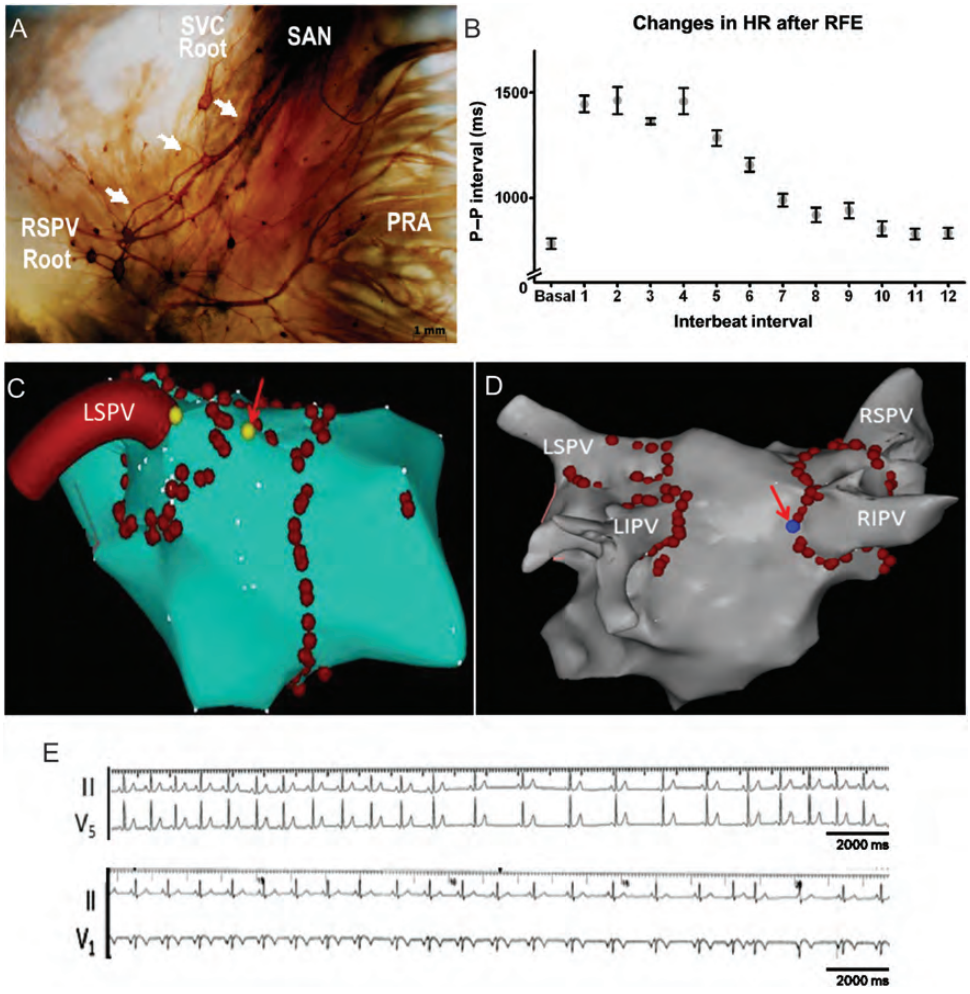

Figure 6 (*A*) Histochemical characterization of human embryonic PV-LA and SAN whole-mount preparations. Ganglia located at the roots of the PVs project nerve fibres (white arrows) to the SAN area. (*B*) Evolution of the P–P interval during control and the first 12 intervals following RFA to the PV roots during sinus rhythm ($n = 5$). Carto maps showing the sites of RFA at the roots of the left superior pulmonary vein (*C*, LSPV) and the right superior pulmonary vein (*D*, RIPV). Red arrows indicate the sites at which RFA induced slowing. (*E*) ECG tracings illustrate the slowing of HR during RFA at the root of the LSPV (top) and the RIPV (bottom). RF current was applied around the PV antrum, power <35 W (<25 W over the posterior LA), temperature <43°C.

stimulation and PVG stimulation + propranolol (*Figure 2B* and *E*). Parasympathetic stimulation causes the rapid activation of the ACh-regulated potassium channels, and the modulation of I_f through the G protein-coupled system.[25] Furthermore, the decrease in HR produced by the stimulation of the PVG indicated that the parasympathetic and sympathetic effects are not simply additive and that parasympathetic slowing of pacemaker rate dominates over sympathetic acceleration.[26,27] In the presence of atropine, an initial decrease in P–P interval was noticeable only with the longest trains of stimulation (*Figure 2C*). This is consistent with the relatively long latency response to sympathetic stimulation[28] compared with vagal.[29]

The time-course of HR change after PVG stimulation (*Figure 3*) indicates that PVG stimulation produced an initial slowing of HR, followed by acceleration around the 10th beat. This suggests that the balance between both autonomic branches shifts from parasympathetic to sympathetic dominance around the 10th beat. This could be explained by three independent factors or a combination thereof: (i) the longer latency of the sympathetic effect, with a delayed response[25]; (ii) a post-synaptic mechanism by which ACh reduces the magnitude of the response to a given adrenergic stimulus[30]; and (iii) the rapid decay in parasympathetic effects once the stimulation ceases due to the rapid breakdown of ACh by acetylcholinesterase.[31]

PVG stimulation in the presence of sympathetic blockade with propranolol caused a sustained decrease in HR after stimulation. The response to parasympathetic stimulation was an instantaneous, maximal increase in P–P interval followed by a gradual decrease towards baseline (*Figure 3*). Conversely, parasympathetic blockade with atropine led to a clear positive chronotropic effect characteristic of sympathetic stimulation (*Figure 3*). After a latency period, the decrease in P–P interval gradually developed (200 ms trains), with the most pronounced effects apparent with the 2000 ms trains. Ng *et al.*[31] found latency periods of 2.9 ± 0.4 and 1.5 ± 0.2 s (at 1 and 7 Hz of sympathetic nerve stimulation, respectively).

It has been suggested that the intrinsic cardiac nervous system is composed of parasympathetic postganglionic and sympathetic neurones.[4,11] However, whether the intrinsic cardiac nervous system is formed only by parasympathetic postganglionic neurones is still debatable.[10] Here, we provide direct evidence demonstrating that the PVG are adrenergic

and cholinergic at both the neuroanatomical and functional levels. HR changes were completely abolished with atropine and propranolol. This argues against a significant role for an alpha adrenergic signalling component.

4.3 Optical mapping of the SAN

PVG stimulation caused shifts in the origin of the SAN pacemaking activity. Several studies have demonstrated that autonomic stimulation can shift the site of earliest activation of the SAN. *In vivo* studies in the dog reported that stimulation of the stellate ganglia and the vagus nerve causes, respectively, cranial and caudal shifts of the site of earliest activation.[32] In isolated rabbit and canine SAN preparations, the site of earliest activation shifted downwards, upwards, or remained the same after nerve stimulation.[33,34] This is in line with what has been recently shown in isolated rabbit and murine SAN preparations subjected to direct high-frequency stimulation or isoproterenol/ACh administration.[18,35] Our study is the first to examine the role of PVG stimulation on the modulation of SAN cycle length and pattern of activation. In our whole-heart experiments, PVG stimulation caused downward (68.2% of cases), or upward (31.8%) displacement of the earliest activation site, where the origin of the activation shifted by 0.80 ± 0.23 mm upwards or 1.14 ± 0.34 mm downwards with respect to control (*Figure 4A–C*). Those results are consistent with the effects of a dominant parasympathetic stimulation, since it has been shown that parasympathetic stimulation with high-frequency stimulation of isolated atrial preparations or ACh infusion produced either an upward or a downward shift in the leading pacemaker site.[18,33–35] The mechanism by which pacemaker shifts occur after parasympathetic stimulation has been studied using numerical simulations.[36] It was proposed that the SAN comprises electrically coupled oscillators (pacemaker cells) with different intrinsic firing rates. Through reciprocal phase-dependent interactions, the coupled oscillators mutually entrain, resulting in the emergence of an origin of activation. Those mutually entrained oscillators, or pacemaker cells, respond to exogenous perturbations such as ACh, through changes in maximum diastolic potential, action potential duration, and cycle length. In the simulations of Michaels *et al.*,[36] ACh caused a downward shift in the dominant pacemaker region, in addition to an increase in the cycle length of the array. By the 10th beat, the array returned to its control pattern and rate of activation. This is similar to the experiments we have carried out (*Figures 3–5*). It has also been suggested that nerve stimulation can produce a pacemaker shift from the centre to the periphery of the SAN because of electrophysiological and neuroanatomical heterogeneities inherent to the SAN.[23,24,34,37]

4.4 Electrophysiological study in patients

It is controversial whether RFA to the PV area during PV isolation can stimulate PVG and produce an increase in the R–R interval, or whether a specifically designed high-frequency stimulation protocol is needed.[15,38–40] The currently proposed mechanism is that slowing of HR is due to the stimulation of the afferent components of the PVG, which in turn evokes a vagal reflex upon the activation of the vagus nerve.[15,38] We were able to observe slowing of HR during PV ablation and quantified the chronotropic response (P–P interval) after RFA to the LSPV and RIPV during sinus rhythm. HR slowed considerably and immediately after RFA delivery. Data from the isolated mouse heart experiments showed a similar behaviour upon stimulation of the PVG, suggesting that the local neuronal circuitry between PVG and the SAN is necessary and sufficient to significantly influence HR.

Although care should always be exerted when attempting to extrapolate experimental findings to the clinical situation, our results in mice nevertheless show that PVG have functional and anatomical biphenotypic characteristics, and that they have significant effects on the electrophysiological control of the SAN without the need of extracardiac neural reflexes. Ablation of the PVG has been proposed for the treatment of atrial fibrillation.[15] However, it has been shown that destruction of PVG can result in the degeneration of ventricular innervation,[41,42] and cardiac autonomic dysfunction has been documented to last for up to a year post-PV isolation.[43] Furthermore, it has been suggested that vagal denervation resulting from AF ablation may predispose to ventricular arrhythmias.[42]

In the context of the overall control of cardiac function, the relevance of the intrathoracic neuronal hierarchy has been shown to be important, and it has become evident that cardiac indexes are affected not only by central neurones but also by a hierarchy of peripheral autonomic neurones (intrinsic cardiac ganglia, intrathoracic extracardiac ganglia) that collectively act to match cardiac output to the body's blood flow demands.[44] Furthermore, it has been suggested that beat-to-beat coordination of regional cardiac indexes is due, in part, to ganglia residing close to the cardiac tissue and constitute the intrinsic cardiac nervous system.[45] This is also evident in the study of Bauer *et al.*,[43] where possible destruction of PVG due to AF ablation affects the autonomic control of HR and HR variability.

On the basis of the studies discussed earlier, and our current experiments, we can speculate that PV ganglia participate in modulating homeostatic HR, independently of the sensory information, the loop reflexes, and also the sympathetic/parasympathetic connections with the central nervous system. More studies will be needed to further substantiate the pathophysiological relevance of these ganglia, and to improve therapeutic interventions targeting the PV region in patients with AF.

Supplementary material

Supplementary material is available at *Cardiovascular Research* online.

Acknowledgements

We thank Richard Karas, Molecular Cardiology Research Institute, Tufts Medical Center, for useful discussions.

Conflict of interest: none declared.

Funding

This work was supported by the Generalitat Valenciana Predoctoral Fellowship BFPI/2008/003, and grants BEFPI/2011/034 and PROMETEO 2010/093 to M.Z., Lithuanian Science Foundation (MIP-074/2011) to K.R. and D.H.P., the Spanish Society of Cardiology and the CNIC foundation to F.A., the Leducq Foundation to J.J., NIH Grants P01-HL039707 and P01-HL087226 to J.J., and R00-HL105574 to S.F.N.

References

1. Johnson TA, Gray AL, Lauenstein JM, Newton SS, Massari VJ. Parasympathetic control of the heart. I. An interventriculo-septal ganglion is the major source of the vagal intracardiac innervation of the ventricles. *J Appl Physiol* 2004;**96**:2265–2272.
2. Rysevaite K, Saburkina I, Pauziene N, Noujaim SF, Jalife J, Pauza DH. Morphologic pattern of the intrinsic ganglionated nerve plexus in mouse heart. *Heart Rhythm* 2011;**8**:448–454.
3. Yuan BX, Ardell JL, Hopkins DA, Armour JA. Differential cardiac responses induced by nicotine sensitive canine atrial and ventricular neurones. *Cardiovasc Res* 1993;**27**:760–769.
4. Rysevaite K, Saburkina I, Pauziene N, Vaitkevicius R, Noujaim SF, Jalife J *et al.* Immunohistochemical characterization of the intrinsic cardiac neural plexus in whole-mount mouse heart preparations. *Heart Rhythm* 2011;**8**:731–738.

5. Pauza DH, Pauziene N, Pakeltyte G, Stropus R. Comparative quantitative study of the intrinsic cardiac ganglia and neurons in the rat, guinea pig, dog and human as revealed by histochemical staining for acetylcholinesterase. *Ann Anat* 2002;**184**:125–136.
6. Pauza DH, Skripka V, Pauziene N. Morphology of the intrinsic cardiac nervous system in the dog: a whole-mount study employing histochemical staining with acetylcholinesterase. *Cells Tissues Organs* 2002;**172**:297–320.
7. Arora RC, Waldmann M, Hopkins DA, Armour JA. Porcine intrinsic cardiac ganglia. *Anat Rec* 2003;**271**:249–258.
8. Gatti PJ, Johnson TA, Massari VJ. Can neurons in the nucleus ambiguus selectively regulate cardiac rate and atrio-ventricular conduction? *J Auton Nerv Syst* 1996;**57**:123–127.
9. Zhuang S, Zhang Y, Mowrey KA, Li J, Tabata T, Wallick DW *et al*. Ventricular rate control by selective vagal stimulation is superior to rhythm regularization by atrioventricular nodal ablation and pacing during atrial fibrillation. *Circulation* 2002;**106**:1853–1858.
10. Chen J, Wasmund SL, Hamdan MH. Back to the future: the role of the autonomic nervous system in atrial fibrillation. *Pacing Clin Electrophysiol* 2006;**29**:413–421.
11. Armour JA. Potential clinical relevance of the 'little brain' on the mammalian heart. *Exp Physiol* 2008;**93**:165–176.
12. Lazzara R, Scherlag BJ, Robinson MJ, Samet P. Selective in situ parasympathetic control of the canine sinoatrial and atrioventricular nodes. *Circ Res* 1973;**32**:393–401.
13. Mick JD, Wurster RD, Duff M, Weber M, Randall WC, Randall DC. Epicardial sites for vagal mediation of sinoatrial function. *Am J Physiol* 1992;**262**:H1401–H1406.
14. Gray AL, Johnson TA, Ardell JL, Massari VJ. Parasympathetic control of the heart II: a novel interganglionic intrinsic cardiac circuit mediates neural control of heart rate. *J Appl Physiol* 2004;**96**:2273–2278.
15. Pappone C, Santinelli V, Manguso F, Vicedomini G, Gugliotta F, Augello G *et al*. Pulmonary vein denervation enhances long-term benefit after circumferential ablation for paroxysmal atrial fibrillation. *Circulation* 2004;**109**:327–334.
16. Miquerol L, Meysen S, Mangoni M, Bois P, van Rijen HV, Abran P *et al*. Architectural and functional asymmetry of the His-Purkinje system of the murine heart. *Cardiovasc Res* 2004;**63**:77–86.
17. Jalife J, Slenter VA, Salata JJ, Michaels DC. Dynamic vagal control of pacemaker activity in the mammalian sinoatrial node. *Circ Res* 1983;**52**:642–656.
18. Fedorov VV, Hucker WJ, Dobrzynski H, Rosenshtraukh LV, Efimov IR. Postganglionic nerve stimulation induces temporal inhibition of excitability in rabbit sinoatrial node. *Am J Physiol Heart Circ Physiol* 2006;**291**:H612–H623.
19. Saburkina I, Pauza DH. Location and variability of epicardiac ganglia in human fetuses. *Anat Embryol (Berl)* 2006;**211**:585–594.
20. Slavikova J, Kuncova J, Reischig J, Dvorakova M. Catecholaminergic neurons in the rat intrinsic cardiac nervous system. *Neurochem Res* 2003;**28**:593–598.
21. Tan AY, Li H, Wachsmann-Hogiu S, Chen LS, Chen PS, Fishbein MC. Autonomic innervation and segmental muscular disconnections at the human pulmonary vein-atrial junction: implications for catheter ablation of atrial-pulmonary vein junction. *J Am Coll Cardiol* 2006;**48**:132–143.
22. Vaitkevicius R, Saburkina I, Rysevaite K, Vaitkeviciene I, Pauziene N, Zaliunas R *et al*. Nerve supply of the human pulmonary veins: an anatomical study. *Heart Rhythm* 2009; **6**:221–228.
23. Mabe AM, Hoover DB. Structural and functional cardiac cholinergic deficits in adult neurturin knockout mice. *Cardiovasc Res* 2009;**82**:93–99.
24. Beau SL, Hand DE, Schuessler RB, Bromberg BI, Kwon B, Boineau JP *et al*. Relative densities of muscarinic cholinergic and beta-adrenergic receptors in the canine sinoatrial node and their relation to sites of pacemaker activity. *Circ Res* 1995;**77**:957–963.
25. Mangoni ME, Nargeot J. Genesis and regulation of the heart automaticity. *Physiol Rev* 2008;**88**:919–982.
26. Brack KE, Coote JH, Ng GA. Interaction between direct sympathetic and vagus nerve stimulation on heart rate in the isolated rabbit heart. *Exp Physiol* 2004;**89**:128–139.
27. Levy MN, Zieske H. Autonomic control of cardiac pacemaker activity and atrioventricular transmission. *J Appl Physiol* 1969;**27**:465–470.
28. Hartzell HC. Regulation of cardiac ion channels by catecholamines, acetylcholine and second messenger systems. *Prog Biophys Mol Biol* 1988;**52**:165–247.
29. Levy MN, Yang T, Wallick DW. Assessment of beat-by-beat control of heart rate by the autonomic nervous system: molecular biology techniques are necessary, but not sufficient. *J Cardiovasc Electrophysiol* 1993;**4**:183–193.
30. Levy MN. Sympathetic-parasympathetic interactions in the heart. *Circ Res* 1971;**29**: 437–445.
31. Ng GA, Brack KE, Coote JH. Effects of direct sympathetic and vagus nerve stimulation on the physiology of the whole heart—a novel model of isolated Langendorff perfused rabbit heart with intact dual autonomic innervation. *Exp Physiol* 2001;**86**:319–329.
32. Goldberg JM. Intra-SA-nodal pacemaker shifts induced by autonomic nerve stimulation in the dog. *Am J Physiol* 1975;**229**:1116–1123.
33. Shibata N, Inada S, Mitsui K, Honjo H, Yamamoto M, Niwa R *et al*. Pacemaker shift in the rabbit sinoatrial node in response to vagal nerve stimulation. *Exp Physiol* 2001;**86**: 177–184.
34. Mackaay AJ, Opthof T, Bleeker WK, Jongsma HJ, Bouman LN. Interaction of adrenaline and acetylcholine on cardiac pacemaker function. Functional inhomogeneity of the rabbit sinus node. *J Pharmacol Exp Ther* 1980;**214**:417–422.
35. Glukhov AV, Fedorov VV, Anderson ME, Mohler PJ, Efimov IR. Functional anatomy of the murine sinus node: high-resolution optical mapping of ankyrin-b heterozygous mice. *Am J Physiol Heart Circ Physiol* 2010;**299**:H482–H491.
36. Michaels DC, Matyas EP, Jalife J. Mechanisms of sinoatrial pacemaker synchronization: a new hypothesis. *Circ Res* 1987;**61**:704–714.
37. Boyett MR, Honjo H, Kodama I. The sinoatrial node, a heterogeneous pacemaker structure. *Cardiovasc Res* 2000;**47**:658–687.
38. Lemery R, Birnie D, Tang AS, Green M, Gollob M. Feasibility study of endocardial mapping of ganglionated plexuses during catheter ablation of atrial fibrillation. *Heart Rhythm* 2006;**3**:387–396.
39. Pokushalov E, Romanov A, Shugayev P, Artyomenko S, Shirokova N, Turov A *et al*. Selective ganglionated plexi ablation for paroxysmal atrial fibrillation. *Heart Rhythm* 2009;**6**:1257–1264.
40. Scherlag BJ, Nakagawa H, Jackman WM, Yamanashi WS, Patterson E, Po S *et al*. Electrical stimulation to identify neural elements on the heart: their role in atrial fibrillation. *J Interv Card Electrophysiol* 2005;**13**:37–42.
41. Puodziukynas A, Kazakevicius T, Vaitkevicius R, Rysevaite K, Jokubauskas M, Saburkina I *et al*. Radiofrequency catheter ablation of pulmonary vein roots results in axonal degeneration of distal epicardial nerves. *Auton Neurosci* 2012;**167**:61–65.
42. Osman F, Kundu S, Tuan J, Jeilan M, Stafford PJ, Andre Ng G. Ganglionic plexus ablation during pulmonary vein isolation – predisposing to ventricular arrhythmias? *Indian Pacing Electrophysiol J* 2010;**10**:104–107.
43. Bauer A, Deisenhofer I, Schneider R, Zrenner B, Barthel P, Karch M *et al*. Effects of circumferential or segmental pulmonary vein ablation for paroxysmal atrial fibrillation on cardiac autonomic function. *Heart Rhythm* 2006;**3**:1428–1435.
44. Ardell JL. Intrathoracic neuronal regulation of cardiac function. In: Armour JA, Ardell JL, eds. *Basic and Clinical Neurocardiology*. New York: Oxford University Press; 2004. p118–152.
45. Armour JA. Functional anatomy of intrathoracic neurons innervating the atria and ventricles. *Heart Rhythm* 2010;**7**:994–996.